

Ezrin, a Membrane Cytoskeleton Cross-Linker Protein, as a Marker of Epithelial Damage in Asthma

Man Jia^{1*}, Xiaoyi Yan^{1,2*}, Xinyu Jiang¹, Yunhui Wu¹, Jiayan Xu¹, Yaqi Meng¹, Yi Yang¹, Xia Shan², Xiuwedi Zhang², Shan Mao³, Wei Gu³, Stelios Pavlidis⁴, Peter J. Barnes⁵, Ian M. Adcock⁵, Mao Huang¹, and Xin Yao¹

¹Department of Respiratory and Critical Care Medicine, the First Affiliated Hospital of Nanjing Medical University, Nanjing, China; ²Department of Respiratory Medicine, Nanjing Jiangning Hospital, Nanjing, China; ³Department of Respiratory Medicine, Nanjing First Hospital, Nanjing, China; ⁴Data Science Institute, Imperial College London, London, United Kingdom; and ⁵Airway Disease Section, National Heart and Lung Institute, Faculty of Medicine, Imperial College London, London, United Kingdom

ORCID IDs: 0000-0003-2101-8843 (I.M.A.); 0000-0002-1301-3631 (X. Yao).

Abstract

Rationale: Bronchial epithelial cell damage occurs in patients with bronchial asthma. Ezrin, a membrane-cytoskeleton protein, maintains cellular morphology and intercellular adhesion and protects the barrier function of epithelial cells.

Objectives: To study the role of ezrin in bronchial epithelial cells injury and correlate its expression with asthma severity.

Methods: Levels of ezrin were measured in exhaled breath condensate (EBC) and serum in patients with asthma and BAL fluid (BALF) from a mouse model of asthma by ELISA. The regulation of IL-13 on ezrin protein levels was studied in primary bronchial epithelial cells. Ezrin knockdown using shRNA was studied in human bronchial epithelial 16HBE cells.

Measurements and Main Results: Ezrin levels were decreased in asthmatic EBC (92.7 ± 34.99 vs. 150.5 ± 10.22 pg/ml, $P < 0.0001$) and serum (700.7 ± 55.59 vs. 279.2 ± 25.83 pg/ml, $P < 0.0001$)

compared with normal subjects. Levels were much lower in uncontrolled ($P < 0.001$) and partly controlled patients ($P < 0.01$) compared with well-controlled subjects. EBC and serum ezrin levels correlated with lung function in patients with asthma and serum ezrin levels were negatively correlated with serum IL-13 and periostin. IL-13-induced downregulation of ezrin expression in primary bronchial epithelial cells was significantly attenuated by the Janus tyrosine kinase 2 inhibitor, TG101348. Ezrin knockdown changed 16HBE cell morphology, enlarged intercellular spaces, and increased their permeability. Ezrin expression was decreased in the lung tissue and BALF of “asthmatic” mice and negatively correlated with BALF IL-13 level.

Conclusions: Ezrin downregulation is associated with IL-13-induced epithelial damage and might be a potential biomarker of asthma control.

Keywords: bronchial asthma; bronchial epithelial cells; IL-13; biomarker

(Received in original form February 26, 2018; accepted in final form October 3, 2018)

*These authors contributed equally to this work.

Supported by the National Natural Science Foundation of China grants 81070025 and 81470237, Jiangsu Health Promotion Project grant ZDRCA2016020, Priority Academic Program Development of Jiangsu Higher Education Institutions grant JX10231802, the Precision Medicine Research of The National Key Research and Development Plan of China (2016YFC0905800), and Jiangsu Senior Personnel Fostering Project grant LGY2016008; I.M.A. and P.J.B. were supported by Wellcome Trust grant 093080/Z/10/Z.

Author Contributions: M.J., I.M.A., and X. Yao designed this study; X.S., X.Z., S.M., and W.G. recruited the patients; M.J., X.J., and Y.Y. collected exhaled breath condensate and serum samples; M.J., X. Yan, and J.X. performed the animal experiments; M.J., Y.W., and Y.M. performed *in vitro* experiments; M.J., X. Yan, and S.P. performed the analysis of data and interpretation; M.J. wrote the manuscript; X. Yao, M.H., I.M.A., and P.J.B. critically revised the manuscript; all authors read and approved the final paper.

Correspondence and requests for reprints should be addressed to Xin Yao, Ph.D., Department of Respiratory & Critical Care Medicine, the First Affiliated Hospital of Nanjing Medical University, 300 Guangzhou Road, Nanjing 210029, China. E-mail: yaixin@njmu.edu.cn.

This article has an online supplement, which is accessible from this issue's table of contents at www.atsjournals.org.

Am J Respir Crit Care Med Vol 199, Iss 4, pp 496–507, Feb 15, 2019

Copyright © 2019 by the American Thoracic Society

Originally Published in Press as DOI: 10.1164/rccm.201802-0373OC on October 5, 2018

Internet address: www.atsjournals.org

At a Glance Commentary

Scientific Knowledge on the

Subject: Bronchial epithelial cell damage occurs in patients with bronchial asthma. However, the underlying molecular mechanisms of IL-13-induced epithelial damage in asthma are unclear.

What This Study Adds to the

Field: This study shows that ezrin levels were decreased in exhaled breath condensate and serum of patients with asthma, and was negatively related to lung function, which might be a potential biomarker of asthma control. The expression of ezrin was downregulated by IL-13 and may be the cause of defective epithelial barrier function in asthma.

Asthma affects at least 300 million people worldwide, and more than 250,000 people die of this disease every year (1). Bronchial asthma is a chronic airway inflammatory disease, involving a variety of cells (including airway structural cells and inflammatory cells) and cytokines (2). Defective epithelial barrier integrity and abnormal epithelial shedding have been reported in asthma, which is important, as airway epithelial cells are the first line of defense against inhaled allergens and environmental exposures in asthma (3). The impaired epithelial barrier may facilitate penetration of environmental allergens, which can subsequently activate innate immune responses and increase asthma severity and susceptibility (4). Moreover, the damaged bronchial epithelium releases inflammatory and growth factors that act on airway smooth muscle cells to alter their function, which leads to airway hyperresponsiveness (5). Importantly, the structural changes occur early in asthma pathogenesis, even years before the appearance of asthma symptoms (6).

Epithelial barrier destruction is associated with reduced mucociliary clearance, decreased cell–cell adhesion, and increased intercellular space and permeability (4). These changes may occur, at least in part, due to chronic inflammation. Epithelial cells are a direct target for IL-13 (7), which causes a reduction in

ciliary beat frequency and in epithelial tight junctions (TJs) (8) and enhances mucus production (7). However, the underlying molecular mechanism of IL-13-induced airway epithelial damage is still not clear.

Epithelial cell–cell and cell–substrate adhesion are dependent upon intracellular junctions by regulating E-cadherin and β -catenin and an orderly arrangement of the cytoskeleton (9). AKAPs (A-kinase anchoring proteins), a family of over 50 scaffold proteins, have been reported to enhance barrier stabilization by coordinate the stabilizing effect of PKA (protein kinase A) on the cellular barrier (10) and interacting with cadherins (11). The ERM (ezrin–radixin–moesin) family can also act as AKAPs (12–14) by building and maintaining the epithelial barrier via connecting transmembrane proteins to the actin cytoskeleton (15). Ezrin (AKAP78), as a constituent of microvilli in regions containing densely packed actin filaments (16), was demonstrated to coprecipitate with β -catenin and E-cadherin (17) in cell–cell and cell–matrix adhesion and regulate tissue architecture by influencing actin assembly (18). By controlling the localization and function of certain apical membrane proteins, ezrin has been implicated in microvillus formation, epithelial cell structure, and polarity (19). Moreover, loss of ERM protein in *Drosophila* results in the damage of mucosal barrier function after the disruption of cellular morphology and the presence of cellular invasion and migration (20). In addition, ezrin has been detected in exosomes released from human

mesothelioma cells, which suggests that ezrin may be secreted through exosomes (21).

We hypothesized that ezrin may be associated with epithelial damage, and might be a potential biomarker for patients with asthma. We aimed to examine ezrin expression and function in bronchial epithelial cells in a murine model of allergic asthma and in patients with asthma.

Methods

Additional detail on the method for making these measurements is provided in the online supplement.

Patient Exhaled Breath Condensate and Serum Collection

Human exhaled breath condensate (EBC) and serum samples were collected from respiratory outpatients with asthma of the First Affiliated Hospital of Nanjing Medical University, Nanjing Jiangning People's Hospital and Nanjing First Hospital, and community healthy volunteers. The EBC was collected by using an EcoScreen condenser (Jaeger) (22). The diagnosis of bronchial asthma and severity of asthma were based on the Global Initiative for Asthma (GINA) guidelines (23). All subjects were nonsmokers. The clinical characteristics of the patients are shown in Table 1. We followed-up six patients who were treated with the combination of low-dose inhaled corticosteroids (budesonide) and rapid-onset long-acting β_2 -agonists (formoterol) in a single inhaler and

Table 1. Baseline Patient Characteristics

Characteristics	Control Group	Asthma Group	P Value
n	23	61	
Sex, male/female	10/13	25/36	0.836
Age, yr	50.88 \pm 1.151	49.35 \pm 1.098	0.6549
BMI, kg/m ²	24.56 \pm 0.851	24.11 \pm 0.582	0.6886
Smoking, pack-years	0	0	
FEV ₁	2.378 \pm 0.063	1.908 \pm 0.123	0.0354*
FEV ₁ % predicted	96.25 \pm 2.390	72.45 \pm 3.469	0.0002 [†]
FEV ₁ /FVC	75.57 \pm 2.178	66.37 \pm 1.683	0.0022 [†]
PEF	5.023 \pm 0.3377	4.192 \pm 0.2939	0.0976

Definition of abbreviations: BMI = body mass index; PEF = peak expiratory flow.

Data are shown as mean \pm SD.

* $P < 0.05$ compared with control groups.

[†] $P < 0.001$ compared with control groups.

[‡] $P < 0.01$ compared with control groups.

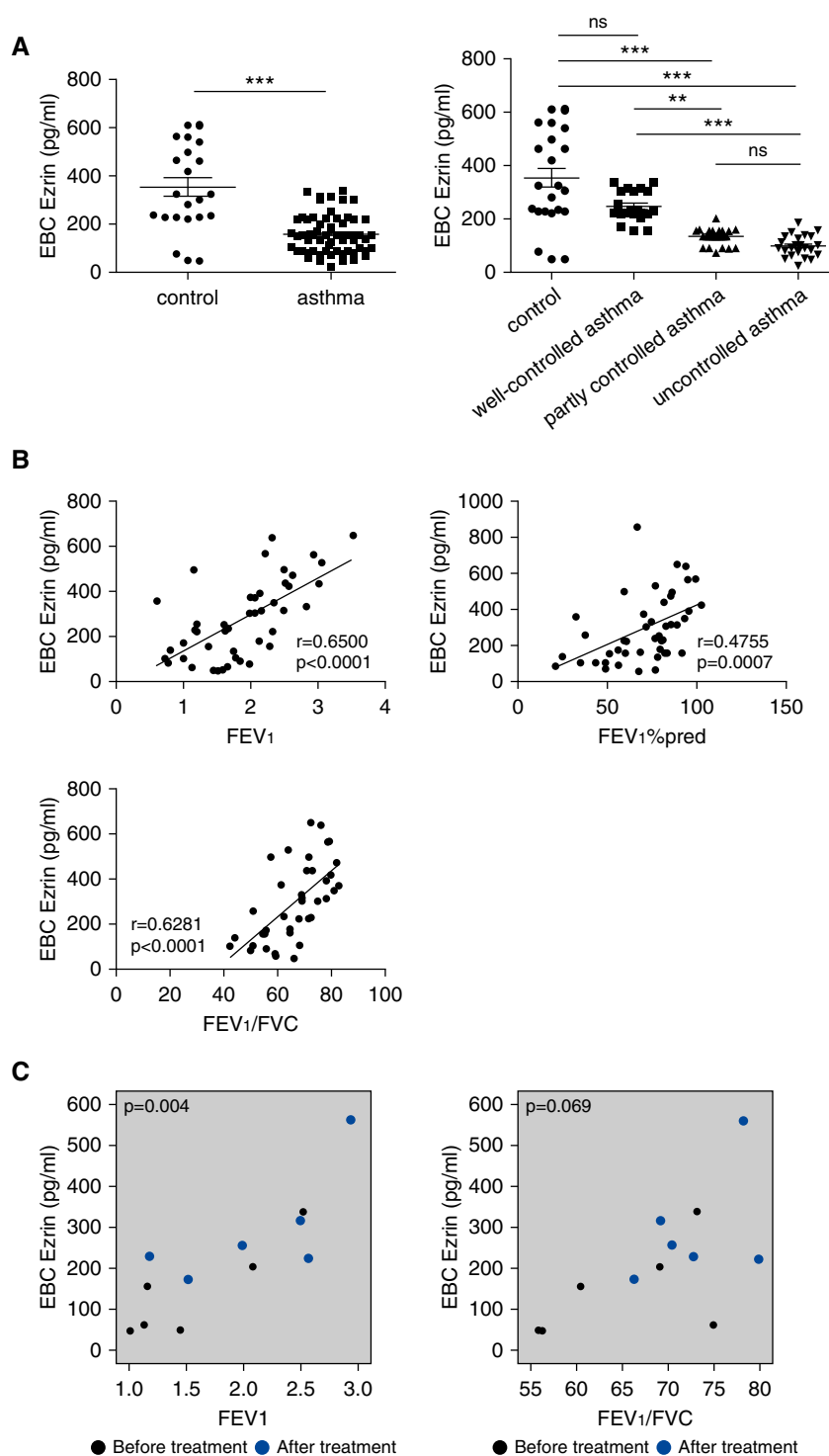


Figure 1. Ezrin expression was decreased in exhaled breath condensate (EBC) of patients with asthma and positively correlated with lung function. (A) Ezrin expression in EBC samples from patients with asthma ($n=56$) and healthy control volunteers ($n=19$) was detected by ELISA. Decreased levels of ezrin were associated with the degree of asthma symptom control according to the asthma control test scores. (B) The relationship between ezrin and FEV₁, FEV₁% predicted, and FEV₁/FVC, $n=40$ –47. (C) Correlation between ezrin EBC levels and FEV₁ and FEV₁/FVC of patients ($n=6$) before and after asthma symptom control using analysis of covariance (ANCOVA). The data were analyzed using Wilcoxon rank-sum test and Kruskal-Wallis test in A, Pearson's correlation test in B. FEV₁%pred = FEV₁% predicted; ns = not significant. ** $P < 0.01$ and *** $P < 0.001$ compared with respective control groups.

recorded their lung function and symptom control. Additional patient serum samples were from the U-BIOPRED (Unbiased Biomarkers for the Prediction of Respiratory Disease Outcomes) study (24). Our study was approved by the Medical Ethics Committee of the First Affiliated Hospital of Nanjing Medical University (no. 2013-SRFA-037).

Animal Experiments

BALB/c mice (6–8 wk old, 20 ± 0.7 g) were randomly divided into four groups: control; ovalbumin (OVA); anti-IgG plus OVA; and anti-IL-13 plus OVA. Protocols for the OVA-induced acute asthma model, as well as an anti-IgG (cat. no. RD AP132P) and an anti-IL-13 (cat. no. RD AF-413-NA) ($30 \mu\text{g}/\text{mouse}$) in an allergic asthma model, were as previously described (25, 26), and are summarized in Figure E1A. Lung tissues were fixed with 4% paraformaldehyde and subsequently embedded in paraffin for immunohistochemistry staining using a rabbit monoclonal anti-ezrin antibody and an anti-E-cadherin antibody (both Cell Signaling Technology Inc.; 1:100) and a rabbit polyclonal anti-ZO-1 antibody (1:100; Proteintech Group Inc.). Hematoxylin and eosin-stained, fixed lung tissue sections were used to assess inflammation.

Cell Culture and Lentivirus shRNA Gene Transfection

Human primary bronchial epithelial cells (PBECs; ScienCell Research Laboratories) and 16HBE cells were cultured as described previously (27, 28). 16HBE cells were transfected with lentiviruses (LVs) encoding for a control shRNA or human ezrin-shRNA-targeting GFP.

Exosomes Isolation and Identification

16HBE cell supernatant underwent sequential preparative ultracentrifugation using a Beckman ultracentrifuge, as previously described (29). Particle size distribution of exosomes was analyzed by nanoparticle tracking analysis by using a ZETASIZER Nano ZS apparatus (Malvern Instruments) and exosomal markers, CD9 and CD63 (Abcam), were also examined by Western blotting.

Transmission Electron Microscopy

Samples (exosomes and ultrathin sections of mouse lung tissue) were prepared as

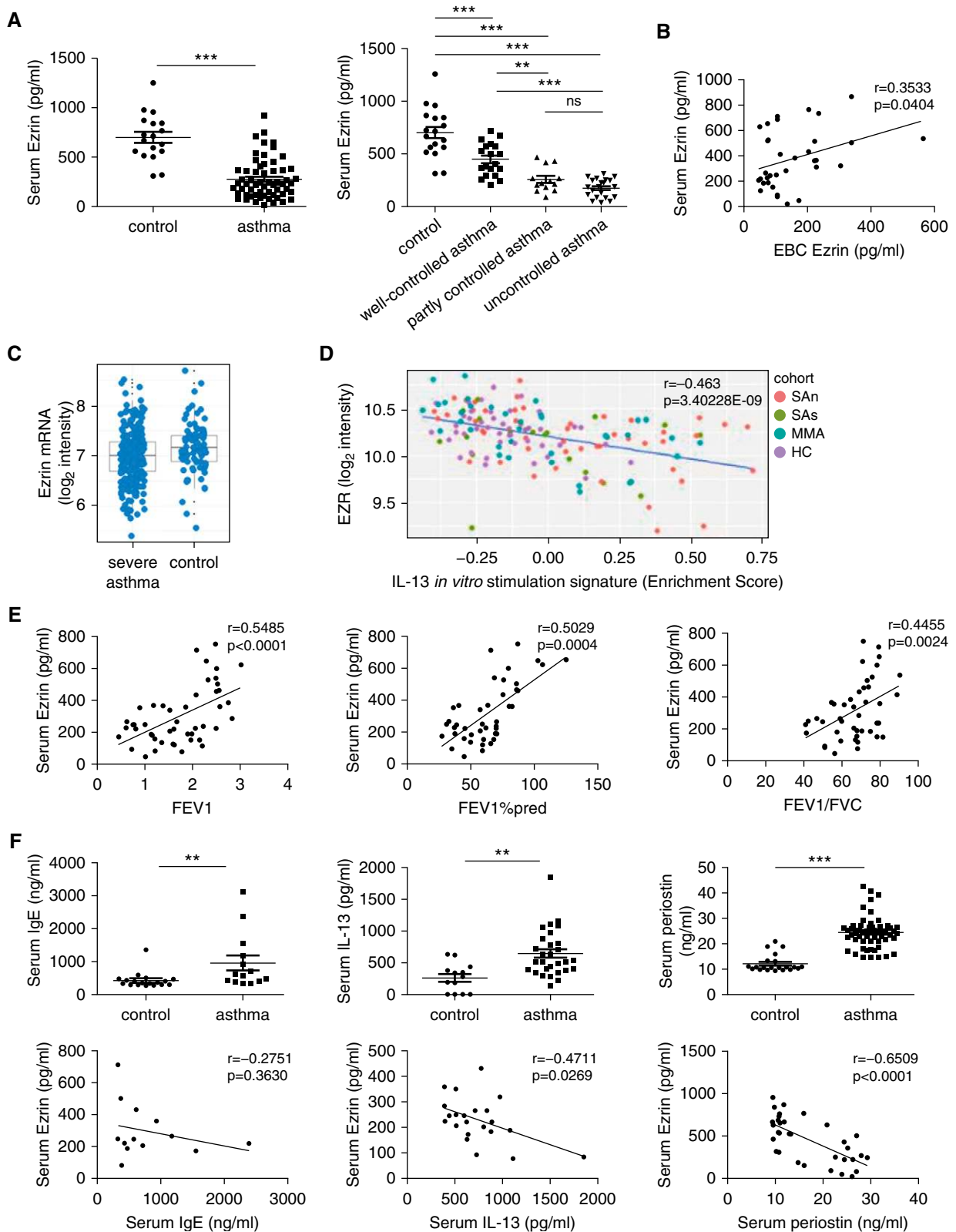


Figure 2. Reduced serum ezrin levels of patients with asthma correlate positively with lung function and negatively with serum IL-13 and periostin levels. (A) The expression of ezrin in serum was reduced in patients with asthma ($n = 59$) compared with healthy control subjects ($n = 18$). Serum levels of ezrin were decreased according to the degree of asthma control: well-controlled group ($n = 19$); partly controlled group ($n = 13$); and uncontrolled group ($n = 23$). (B) The correlation between ezrin levels in exhaled breath condensate (EBC) and in serum ($n = 34$). (C) Ezrin mRNA expression in blood cells in severe

described previously (29, 30) and were photographed under transmission electron microscopy (JEOL-1010; Jeol).

ELISA

The levels of IL-4, IL-5, IL-13 (R&D Systems), and ezrin in mouse BAL fluid (BALF; CSB-EL007914MO; Cusabio) and human serum ezrin (SEB297Hu; Cloud Clone Corp.), IL-13, periostin, and IgE were measured by ELISA kit, according to the manufacturer's instructions.

Measurement of Transepithelial Electrical Resistance and Epithelial Permeability

Transepithelial electrical resistance (TER) of the 16HBE cells, grown in 24-well Transwell (Corning Costar) inserts, was measured daily using the Millicell-ERS system (Millipore Co.) (31). Paracellular flux across the epithelium was measured using fluorescein isothiocyanate-labeled 4-kD dextran (0.5 mg/ml) (Sigma-Aldich) added to the upper chamber followed by incubation for 2 hours at 37°C.

Statistical Analysis

All data are presented as mean (\pm SEM), and P less than 0.05 was considered significant. The statistical analyses were performed using GraphPad Prism software v5.0 (GraphPad Software, Inc.). Experiments with multiple comparisons were evaluated by one-way ANOVA followed by Student-Newman-Keuls *post hoc* test or Bonferroni's *post hoc* test (normally distributed parameters) and Kruskal-Wallis test (nonnormally distributed parameters) for multiple data sets. Comparisons between two groups were performed with an unpaired Student's t test for normally distributed parameters and with Wilcoxon rank-sum test for nonnormally distributed parameters.

Results

Ezrin Expression Was Decreased in EBC of Patients with Asthma and Positively Correlated with Lung Function

Ezrin concentrations in EBC were significantly reduced in patients with asthma (150.5 ± 10.22 pg/ml) compared with normal subjects (392.7 ± 34.99 pg/ml) (Figure 1A). Ezrin concentrations decreased according to asthma control: well-controlled group (243.8 ± 15.36 pg/ml); partly controlled group (133.6 ± 9.08 pg/ml); and uncontrolled group (98.13 ± 8.38 pg/ml). Subjects with poor symptom control had a 1.92-fold-lower level of ezrin in EBC than those with well-controlled asthma (Figure 1A). Ezrin levels in EBC correlated positively with lung function (FEV_1 , $FEV_1\%$ predicted, and FEV_1/FVC) as a measure of airway obstruction (Figure 1B). In a substudy, we found that ezrin EBC levels were increased, accompanying the improvement in lung function seen in six patients after treatment with combination therapy (Figure 1C).

Reduced Serum Ezrin Levels of Patients with Asthma Correlate Positively with Lung Function and Negatively with Serum IL-13 and Periostin Levels

The serum levels of ezrin in patients with asthma were significantly decreased (279.2 ± 25.83 pg/ml) compared with healthy control subjects (700.7 ± 55.59 pg/ml), and successively decreased in well-controlled (446.1 ± 35.54 pg/ml), partly controlled (256.3 ± 32.35 pg/ml), and uncontrolled asthma (174.5 ± 16.73 pg/ml) (Figure 2A). Subjects with poor symptom control had a 3.77-fold-lower level of serum ezrin than those with well-controlled asthma. We validated the reduction in ezrin expression in asthma in the U-BIOPRED cohort, which

demonstrated a significant reduction in ezrin mRNA expression in blood cells in severe asthma compared with healthy control subjects (false discovery rate = 1.59×10^{-5}) (Figure 2C). Ezrin gene expression was negatively correlated ($r = -0.463$, adjusted $P = 3.40228E-09$) with the enrichment score of IL-13-stimulated epithelial cell-derived T2 signature genes in patients with asthmatic (severe, nonsevere) patients and healthy subjects (Figure 2D). However, there was no impact of corticosteroid use on ezrin expression in the U-BIOPRED cohort (data not shown). In our study, ezrin levels in serum were positively related to levels of EBC ezrin (Figure 2B) and lung function (FEV_1 , $FEV_1\%$ predicted, and FEV_1/FVC) (Figure 2E). The level of serum IgE (2.24-fold; 959.7 ± 228.2 vs. 427.8 ± 59.12 ng/ml), IL-13 (2.44-fold; 642.8 ± 68.05 vs. 263.3 ± 62.57 pg/ml), and periostin (2.01-fold; 24.41 ± 0.82 vs. 12.13 ± 0.68 ng/ml) were increased in patients with asthma compared with healthy control subjects. Serum ezrin was negatively correlated with IL-13 and periostin, although not related to IgE (Figure 2F).

Ezrin Is Expressed on Exosomes Secreted by Bronchial Epithelial Cells

The electron microscopic images showed vesicles derived from 16HBE supernatant with the characteristic cup-shape morphology of exosomes (Figure 3A). The mean size distribution was 124 nm, and the percentage of particles between 20 and 200 nm was 84.3% (Figure 3B), which corresponds to the exosome size. Western blotting analysis was performed on exosome lysates from the culture supernatants. As depicted in Figure 3C, the exosome markers, CD63 (53 kD) and CD9 (25 kD) proteins, were detected. All these results confirm the presence of exosomes in bronchial epithelial cell culture supernatants. We further isolated exosomes derived

Figure 2. (Continued). asthma compared with healthy control subjects, by cohort (adjusted $P = 0.0022$). Graphs are expressed as \log_2 intensity robust multiarray average signals. The differences between healthy control subjects and patients with severe asthma were analyzed using the Benjamini-Hochberg method for adjusted P value/false discovery rate. (D) The correlation between EZR expression and T2 signature gene expression in IL-13-stimulated epithelial cells from patients with asthma and healthy subjects ($n = 147$). Ezrin gene expression is presented as \log_2 intensity robust multiarray average signals and the expression of the IL-13 signature genes as an enrichment score. (E) The relationship between serum ezrin and FEV_1 , $FEV_1\%$ predicted, and FEV_1/FVC ($n = 44-47$). (F) The concentrations of serum IgE (asthma group, $n = 18$; control group, $n = 14$), IL-13 (asthma group, $n = 29$; control group, $n = 13$), and periostin (asthma group, $n = 56$; control group, $n = 23$) were measured using ELISA (upper panels), and their relationships with ezrin were also analyzed (lower panels). Data were quantified and expressed as mean \pm SD. ** $P < 0.01$ and *** $P < 0.001$ compared with respective control subjects. The data were analyzed using Wilcoxon rank-sum test (A), IgE and periostin (F), Student's t test in IL-13 (F), and Pearson's correlation test (B and D-F). EZR = ezrin; $FEV_1\%$ pred = $FEV_1\%$ predicted; HC = healthy nonsmoking control subjects; MMA = mild/moderate nonsmoking asthma; ns = not significant; SAn = severe nonsmoking asthma; SAs = smokers with severe asthma.

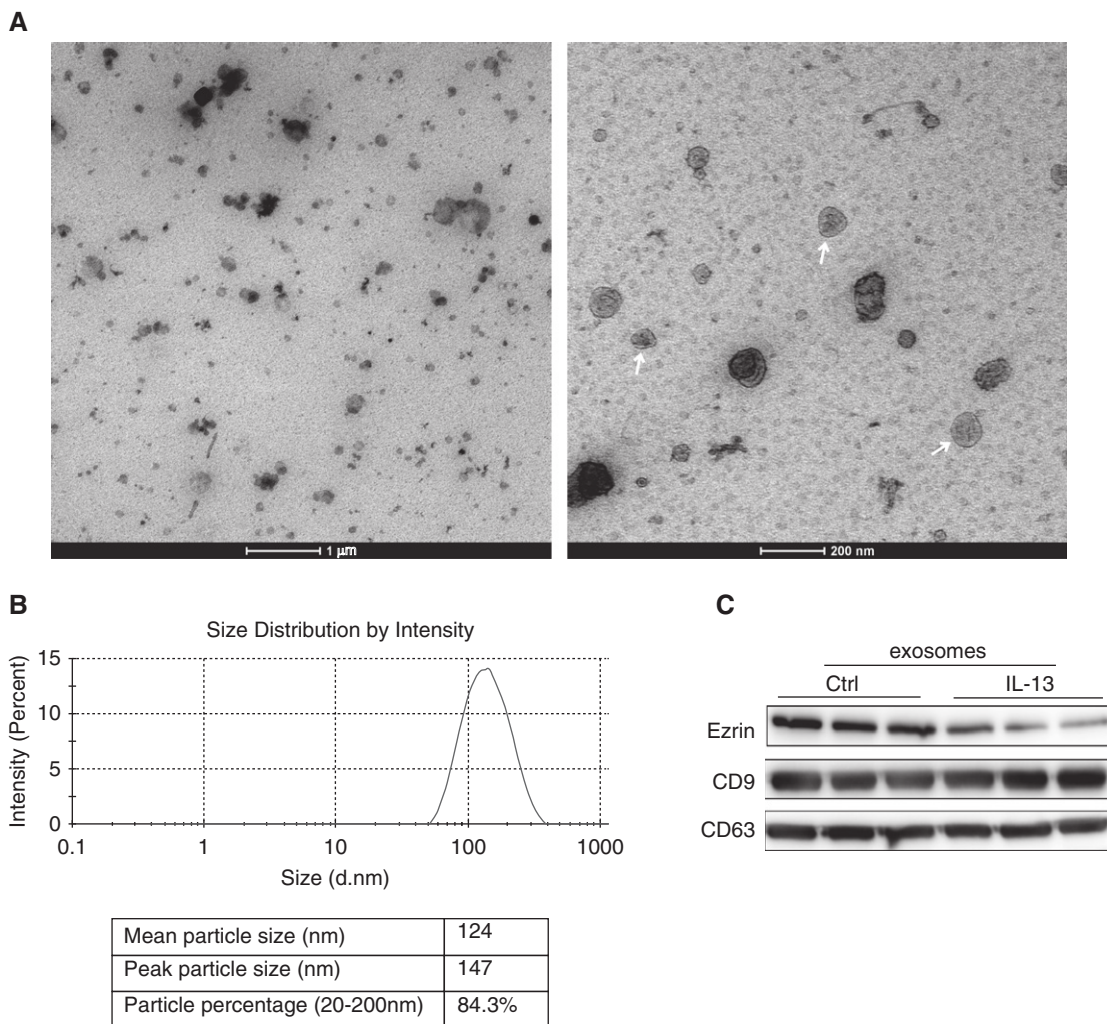


Figure 3. Ezrin is expressed on exosomes secreted by bronchial epithelial cells. (A) Electron microscopic observation of whole-mounted exosomes purified from 16HBE cells. White arrows indicate exosomes. Scale bars = 1 μm (left panel) and 200 nm (right panel). (B) Intensity and size distribution of exosomes derived from 16HBE cells were measured by nanoparticle tracking analysis. Graph showing the average percentage of particles within 50- to 350-nm size in exosome. (C) Western blot analysis showed the presence of ezrin as well as exosome markers, CD9 and CD63, in exosomes isolated from 16HBE cells (Ctrl) and the IL-13 (30 ng/ml)-treated group (IL-13).

from supernatant of IL-13-treated 16HBE cells, and found that ezrin protein was expressed on exosomes and was decreased compared with control group (Figure 3C), which suggests that ezrin is likely to be secreted via exosomes under the influence of IL-13.

IL-13 Downregulates Ezrin Expression in Bronchial Epithelial Cells by the Janus Tyrosine Kinase 2/Signal Transducer and Activator of Transcription 6 Pathway

We examined the effect of the T-helper cell type (Th) 2 cytokines, IL-4 and IL-13, and the Th1 cytokine, TNF- α , on ezrin mRNA and protein expression in 16HBE cells.

IL-13 markedly reduced the expression of ezrin mRNA (reduced by 48.2%) and protein (reduced by 45.7%), whereas a similar observation was made for IL-4 effects on ezrin mRNA and protein levels (reduced by 41.6% and 27.4%, respectively) (Figures 4A and 4B). TNF- α had no significant effect on the ezrin mRNA and enhanced ezrin protein expression at 24 hours only (Figures 4A and 4B). A similar effect of IL-13 on reducing ezrin protein expression was seen in PBECs (Figure 4C).

To explore molecular mechanism for IL-13-mediated ezrin, PBECs were treated with IL-13 for 1 hour. IL-13 induced phosphorylation of JAK2 (Janus kinase 2) (p-JAK2), followed by an increase of its

downstream p-STAT6 (phosphorylated signal transducer and activator of transcription 6) nuclear translocation, and subsequently leading to inhibition of ezrin protein expression; however, the effect was reversed by pretreatment of PBECs with the JAK2 inhibitor TG101348 (Figure 4C). These data suggest that IL-13-induced downregulation of ezrin in bronchial epithelial cells is due, at least in part, to a JAK2/STAT6-dependent pathway.

Ezrin Depletion Alters Cell Morphology and Increases Cellular Permeability

To determine whether the decrease in ezrin expression induced by IL-13 was associated

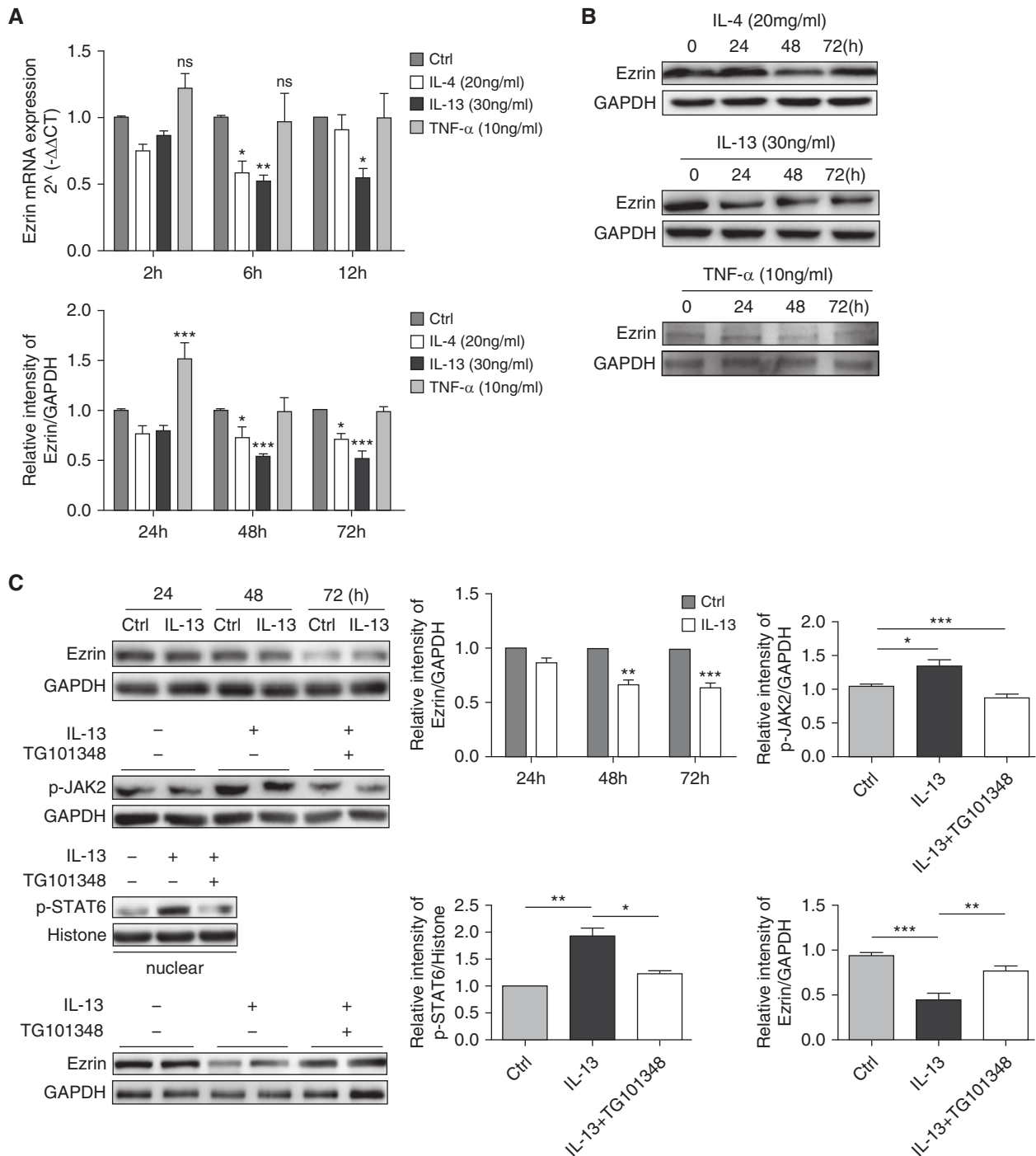


Figure 4. IL-13 downregulates ezrin expression in bronchial epithelial cells via the JAK2 (Janus tyrosine kinase 2)/STAT6 (signal transducer and activator of transcription) pathway. (A) 16HBE cells were treated with IL-4 (20 ng/ml), IL-13 (30 ng/ml), and TNF- α (10 ng/ml) for 2, 6, and 12 hours, and ezrin mRNA expression was measured by quantitative RT-PCR. (B) 16HBE cells were exposed to IL-4 (20 ng/ml), IL-13 (30 ng/ml), and TNF- α (10 ng/ml) for 24, 48, and 72 hours, and ezrin protein production was determined by Western blotting. (C) Primary bronchial epithelial cells (PBECs) were stimulated with IL-13 (30 ng/ml) for 24, 48, and 72 hours. Ezrin protein was evaluated by Western blotting. PBECs were pretreated with the JAK2 inhibitor TG101348 (30 nM) for 1 hour before IL-13 (30 ng/ml) stimulation (1 h). The total phospho (p)-JAK2 protein level and p-STAT6 protein level in the nucleus were measured by Western blotting. The effect of TG101348 pretreatment on IL-13-regulated ezrin expression was evaluated by Western blotting. Data are presented as mean \pm SEM of three independent experiments using one-way ANOVA followed by Student-Newman-Keuls *post hoc* analysis. ns = not significant. * P < 0.05, ** P < 0.01 and *** P < 0.001, compared with control (Ctrl). TNF- α = tumor necrosis factor- α .

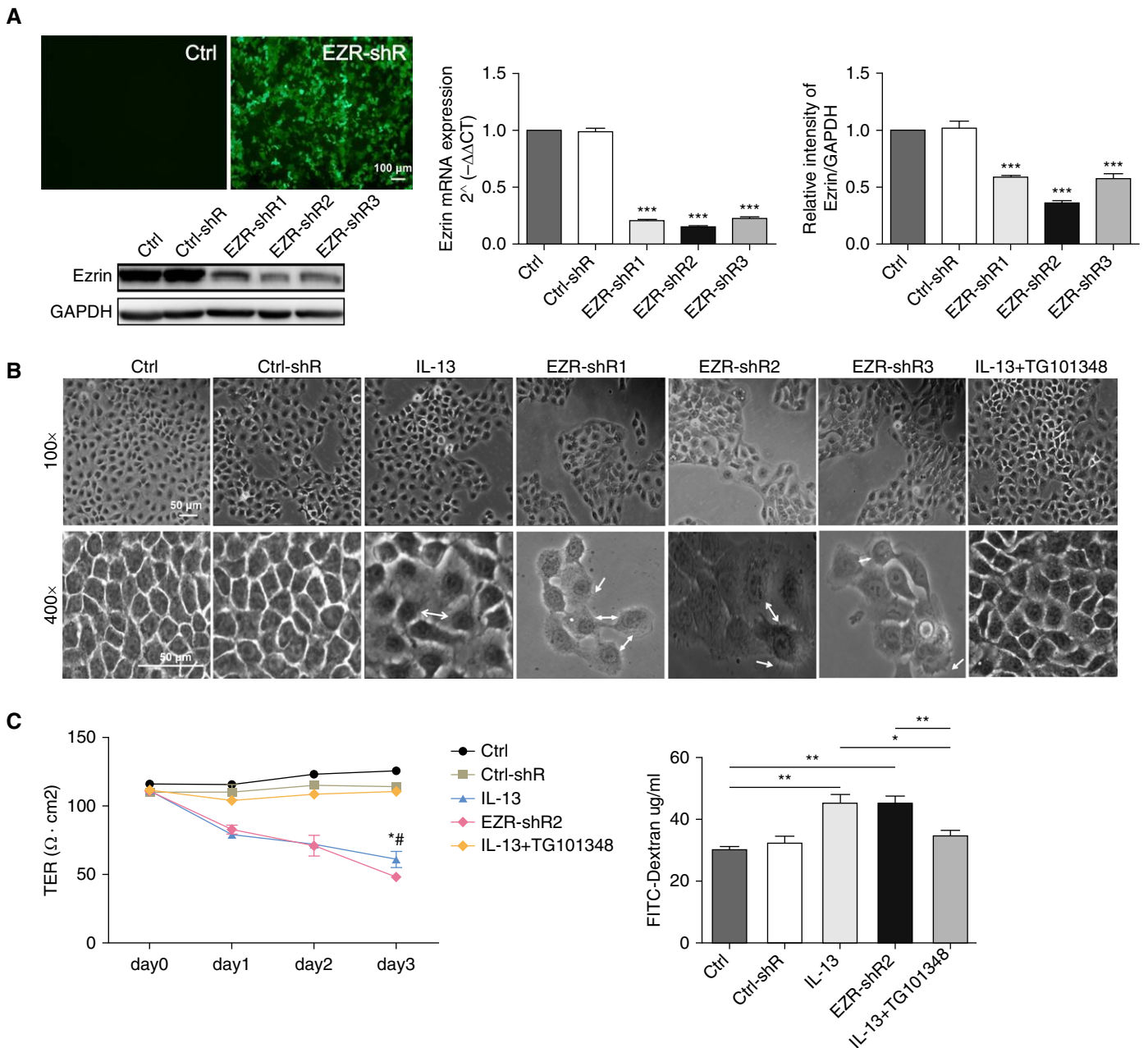


Figure 5. Ezrin depletion alters cell morphology and increases cellular permeability. (A) 16HBE cells were transfected with lentiviruses encoding for a control shRNA (Ctrl) or human ezrin-shRNA (EZR-shR1–3) tagged with GFP for 24 hours and then washed, and the cells were examined after a further 48 hours. GFP was detected by immunofluorescence (scale bar = 100 μm), quantitative RT-PCR, and Western blotting. *** $P < 0.001$ compared with the control group. (B) Phase-contrast images (original magnification, $\times 100$ and $\times 400$; scale bars = 50 μm) of 16HBE cells treated with control media (Ctrl), transfection control (Ctrl-shR), IL-13 (30 ng/ml), ezrin-shRNA (EZR-shR1–3), and IL-13 (30 ng/ml) + TG101348 (30 nM). White double-headed arrows show intercellular space enlargement; white single arrows show cellular protrusions. (C) Assessment of the permeability of the bronchial epithelium based on transepithelial electrical resistance (TER) (left panel) and fluorescein isothiocyanate (FITC)-dextran (right panel) in control media (Ctrl), transfection control (Ctrl-shR), IL-13 (30 ng/ml), ezrin-shRNA (EZR-shR2), and IL-13(30 ng/ml) + TG101348 (30 nM) groups. The data were analyzed using one-way ANOVA followed by Student-Newman-Keuls *post hoc* analysis. (C) Left panel: * $P < 0.05$ (IL-13 vs. control), # $P < 0.05$ (EZR-shR2 vs. Ctrl-shR); right panel: * $P < 0.05$ and ** $P < 0.01$ compared with respective control subjects. Phase-contrast images are representative of those seen in three independent experiments.

with the damage of bronchial epithelial cells, ezrin expression was knocked down in 16HBE cells using LV-shRNA. Ezrin was successfully transfected with LVs encoding

GFP (Figure 5A), resulting in knockdown of ezrin mRNA (Figure 5A) and protein levels (Figure 5A). Ezrin-shRNA2 was the most effective shRNA, with a knockdown

efficiency of 80% for mRNA and 70% for protein.

Knockdown of ezrin using LV-shRNAs 1–3 could all result in marked morphological

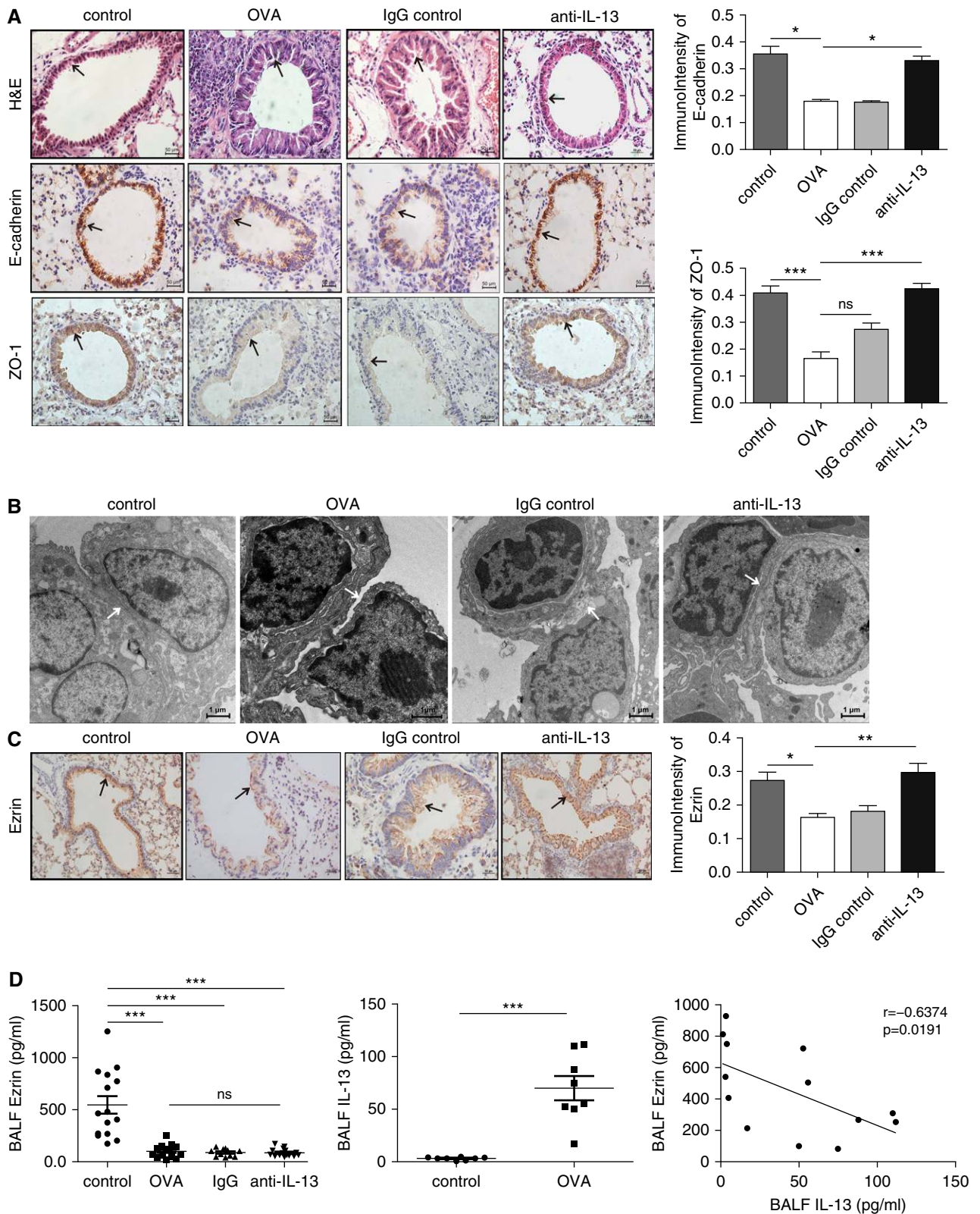


Figure 6. Ezrin expression and epithelial cell-cell adhesion were decreased in an ovalbumin (OVA)-treated allergic mouse model of asthma and restored by anti-IL-13 treatment. (A) Hematoxylin and eosin (H&E) staining of lung tissue in “asthma mice” (black arrows indicate bronchial epithelial cells). Representative image of E-cadherin and ZO-1 immunostaining (black arrows in the middle and bottom panels indicate their expression on the bronchial epithelial cells) was examined in saline-exposed control mice (control), OVA-treated mice (OVA), OVA + anti-IgG antibody-treated mice (anti-IgG), and OVA + anti-IL-13 antibody-treated mice (anti-IL-13), and was

changes in 16HBE cells. This changed from a typical multilateral paving stone-like appearance to a round or fusiform appearance accompanied by protrusions from the cells (Figure 5B). Furthermore, the TER of bronchial epithelial cells was significantly decreased, from 120.1 (± 2.51) to 78.21 (± 2.51) Ω cm² and the intercellular space and permeability were increased after ezrin depletion, which was similar to that seen with IL-13 treatment. However, these impaired features could be alleviated with TG101348 pretreatment (Figures 5B and 5C).

Ezrin Expression and Epithelial Cell–Cell Adhesion Were Decreased in a Mouse Model of Asthma and Prevented by Anti-IL-13 Treatment in Lung Tissue

To further confirm the involvement of IL-13 in epithelial damage of allergic asthma, we established an allergic asthma and an anti-IL-13-in-allergic-asthma model (see Figure E1 in the online supplement). OVA significantly thickened the trachea wall, widened intercellular space, and enhanced inflammatory cell infiltration, which was attenuated by anti-IL-13 antibody treatment (Figure 6A). The epithelial cell–cell adherence was clearly damaged in the allergic asthma model, whereas prophylactic treatment with a neutralizing IL-13 antibody alleviated the destruction of the cellular TJs (Figure 6B). In addition, the expression of TJ marker, ZO-1, and of the adherens junction marker, E-cadherin, were both decreased in the lung of mice with allergic asthma (Figure 6A). These changes were not seen in the anti-IL-13 antibody-treated animals (Figures 6A and 6B).

Ezrin expression was localized to the apical membrane of bronchial epithelial cells and clearly reduced in “asthma mice” (Figures 6C). Ezrin levels were also suppressed in the BALF of “asthmatic mice” (205.9 ± 34.71 pg/ml) compared with controls ($1,099 \pm 166.1$ pg/ml), and were negatively correlated with increased

BALF IL-13 ($r = -0.6374$, $P = 0.0191$) (Figure 6D). However, there was no significant difference in BALF ezrin expression between “asthmatic mice” and anti-IL-13 antibody-treated mice (173.6 ± 19.64 pg/ml; Figure 6D).

Discussion

We demonstrated that ezrin levels in serum and EBC were reduced in subjects with asthma compared with healthy control subjects, and were correlated positively with lung function. In contrast, serum ezrin was negatively correlated with serum IL-13 and periostin. We demonstrated that IL-13 downregulated ezrin levels in airway epithelial cells, and that this was mediated by the JAK2/STAT6 signaling pathway. Knockdown of ezrin in bronchial epithelial cells had a similar effect on epithelial damage, including increased intercellular space and permeability, as seen with IL-13, which implicates ezrin in this important aspect of asthma pathogenesis. Moreover, we discovered that ezrin could be secreted from airway epithelial cells via exosomes under the influence of IL-13. In an animal model of allergic asthma, OVA challenge resulted in decreased ezrin expression and epithelial cell–cell adhesion in lung tissue, and this was prevented by anti-IL-13 treatment. These results indicated that decreased ezrin, due to IL-13, may be the cause of defective epithelial barrier in asthma, and may be a potential biomarker of asthma airway epithelial cell dysfunction or remodeling.

Ezrin was initially identified as a cross-linker between the plasma membrane and the cortical cytoskeleton (16). It is highly enriched and colocalizes with actin at the apical surface of many types of simple epithelial cells that have microvilli (32, 33). Based on its localization and protein-binding activity, ezrin has been implicated in regulating a variety of cellular processes, including cell polarity (34), epithelial morphology (18), and cell–cell and

cell–substrate adhesion (35, 36), all of which are essential for maintenance of epithelial barrier integrity.

Ezrin protein maintains a dormant, inactive conformation through masking of the interaction between its FERM (band 4.1, ERM) and the C-terminal domains in the cytoplasm (15). Activation of ezrin is triggered by phosphorylation at certain residues: threonine residue (Thr567 in ezrin) through p38 MAPK (mitogen-activated protein kinase)- and PKC-dependent mechanisms (36, 37) or of tyrosine residues (Tyr353 in ezrin) driven by the JNK (c-Jun N-terminal kinase)/MKK7 (mitogen-activated protein kinase kinase 7) pathway (38). JAK2, consisting of a FERM domain and an atypical Src homology 2 domain, is an indispensable regulator in IL-13/STAT6 signaling pathways (39). A previous study also indicated that ezrin may be a downstream target of the receptor tyrosine kinase (40). In our study, downregulation of ezrin was accompanied by JAK2/STAT6 activation in response to IL-13, and was reversed after using a selective JAK2 inhibitor, TG101348 (Fedratinib; SAR302503) (41).

Previous studies have reported that IL-13 may repress ezrin binding to the apical cytoskeleton, and thereby suppress ciliary function via a STAT6-mediated attenuation of foxj1 expression (42, 43). Our data extend the mechanisms of IL-13 suppression of ezrin expression and function by indicating a direct transcriptional effect mediated by the JAK2/STAT6 pathway. Thus, IL-13 may control ciliary function by these two processes acting together to control both ezrin expression and function.

IL-13 alters mucociliary differentiation and ciliary beating of human airway epithelial cells, and also increases the proportion of secretory cells (7, 8). We have extended the understanding of IL-13 function to show that IL-13–induced epithelial damage was accompanied by paracellular gap formation, decreased cellular TJ and TER, as well as increased permeability to fluxes of dextran *in vitro*

Figure 6. (Continued). analyzed by Image-Pro Plus 6.0. Scale bars, 50 μ m. (B) Epithelial cell–cell adherence was determined by electron microscopy (scale bars, 1 μ m; white arrow). (C) Immunohistochemical analysis of ezrin expression in saline-exposed control mice (control), OVA-treated mice (OVA), OVA + anti-IgG antibody-treated mice (anti-IgG), and OVA + anti-IL-13 antibody-treated mice (anti-IL-13) (original magnification, $\times 400$; scale bar = 100 μ m; black arrow) and scored (right graph). (D) The concentrations of ezrin in BAL fluid (BALF) of OVA-treated mice (OVA), OVA + anti-IgG antibody-treated mice (anti-IgG), and OVA + anti-IL-13 antibody-treated mice (anti-IL-13), and IL-13 of asthma mice and controls were measured using an ELISA. The data are presented as mean \pm SEM and were analyzed by Student's *t* test (control group, $n = 8-15$; asthma group; $n = 8-17$). The correlation between ezrin and IL-13 in BALF of mice was analyzed by Pearson's correlation test. ns = not significant. * $P < 0.05$, ** $P < 0.01$, and *** $P < 0.001$ compared with respective controls.

and *in vivo*. Ezrin knockdown had similar effects on IL-13, which suggests that ezrin may be an important player in IL-13–induced epithelial injury.

Previous studies have demonstrated that IL-13 can influence the release of exosomes from bronchial epithelial cells, which are the major source of exosomes in the lungs of patients with asthma (44). In addition to human mesothelioma cells (21), ezrin expression on exosome-like vesicles from ram epididymal fluid and boar seminal plasma has been detected (45, 46), which indicates that ezrin can be secreted through exosomes. We show here that ezrin could be secreted from bronchial epithelial cells via exosomes, and that this was decreased under the influence of IL-13. Furthermore, ezrin levels, both in BALF of asthma mice and serum samples of patients with asthma, were negatively correlated with IL-13, which all suggest that IL-13 may also have an inhibitory effect on secretion of ezrin.

A study has recently shown that the expression of ezrin might be different in pulmonary diseases. The expression of ezrin

protein was unaltered in the BALF of patients with COPD, but was elevated threefold in patients with lung cancer compared with control subjects (47).

However, in our study, serum ezrin was decreased in patients with asthma, and negatively associated with biomarkers of Th2 airway inflammation periostin (48) and IL-13 (49), which were both increased in our patients with asthma. Ezrin gene expression was negatively correlated with the T2 signature (50) derived from IL-13–stimulated epithelial cells. This relationship indicated that ezrin may be a marker of Th2 phenotype that manifests clinical features of asthma. A limitation to this study is that we did not formally measure the Th2 status of all patients with asthma studied. EBC and serum ezrin both had a negative relationship with lung function, and ezrin measurements may be useful in patients in whom it is not possible to obtain lung function measures (50).

There are some limitations to this study. Although anti-IL-13 prevented the

changes in ezrin expression in lung tissue and function, this study was performed prophylactically, and the effect of therapeutic intervention is unknown. We believe that ezrin should be considered as a biomarker that can indicate both epithelial injury and control levels in patients with asthma. The potential of using ezrin levels to monitor or dictate clinical practice need to be further investigated with appropriately designed prospective studies. Future studies will investigate the mechanism by which ezrin is secreted by exosomes and whether autologous exosomes will enable ezrin to treat epithelial damage. ■

Author disclosures are available with the text of this article at www.atsjournals.org.

Acknowledgment: The authors thank Dr. Fang Wang (the principal investigator of the Laboratory of Cardiovascular Disease of the First Affiliated Hospital, Nanjing Medical University) and Dr. Jifu Wei (the principal investigator of the Research Division of Clinical Pharmacology of the First Affiliated Hospital of Nanjing Medical University) for technical support.

References

- Bousquet J, Mantzouranis E, Cruz AA, Ait-Khaled N, Baena-Cagnani CE, Bleecker ER, *et al*. Uniform definition of asthma severity, control, and exacerbations: document presented for the World Health Organization Consultation on Severe Asthma. *J Allergy Clin Immunol* 2010;126:926–938.
- Cohn L, Elias JA, Chupp GL. Asthma: mechanisms of disease persistence and progression. *Annu Rev Immunol* 2004;22:789–815.
- Holgate ST, Roberts G, Arshad HS, Howarth PH, Davies DE. The role of the airway epithelium and its interaction with environmental factors in asthma pathogenesis. *Proc Am Thorac Soc* 2009;6:655–659.
- Xiao C, Puddicombe SM, Field S, Hayward J, Broughton-Head V, Puxeddu I, *et al*. Defective epithelial barrier function in asthma. *J Allergy Clin Immunol* 2011;128:549–56.e1, 12.
- Barnes PJ, Cuss FM, Palmer JB. The effect of airway epithelium on smooth muscle contractility in bovine trachea. *Br J Pharmacol* 1985;86:685–691.
- Barbato A, Turato G, Baraldo S, Bazzan E, Calabrese F, Panizzolo C, *et al*. Epithelial damage and angiogenesis in the airways of children with asthma. *Am J Respir Crit Care Med* 2006;174:975–981.
- Cohn L, Homer RJ, Marinov A, Rankin J, Bottomly K. Induction of airway mucus production by T helper 2 (Th2) cells: a critical role for interleukin 4 in cell recruitment but not mucus production. *J Exp Med* 1997;186:1737–1747.
- Laoukili J, Perret E, Willems T, Minty A, Parthoens E, Houcine O, *et al*. IL-13 alters mucociliary differentiation and ciliary beating of human respiratory epithelial cells. *J Clin Invest* 2001;108:1817–1824.
- Steed E, Balda MS, Matter K. Dynamics and functions of tight junctions. *Trends Cell Biol* 2010;20:142–149.
- Schlegel N, Waschke J. VASP is involved in cAMP-mediated Rac 1 activation in microvascular endothelial cells. *Am J Physiol Cell Physiol* 2009;296:C453–C462.
- Oldenburger A, Poppinga WJ, Kos F, de Bruin HG, Rijks WF, Heijink IH, *et al*. A-kinase anchoring proteins contribute to loss of E-cadherin and bronchial epithelial barrier by cigarette smoke. *Am J Physiol Cell Physiol* 2014;306:C585–C597.
- Dransfield DT, Bradford AJ, Smith J, Martin M, Roy C, Mangan PH, *et al*. Ezrin is a cyclic AMP-dependent protein kinase anchoring protein. *EMBO J* 1997;16:35–43.
- Semenova I, Ikeda K, Ivanov P, Rodionov V. The protein kinase A-anchoring protein moesin is bound to pigment granules in melanophores. *Traffic* 2009;10:153–160.
- Deming PB, Campbell SL, Stone JB, Rivard RL, Mercier AL, Howe AK. Anchoring of protein kinase A by ERM (ezrin-radixin-moesin) proteins is required for proper netrin signaling through DCC (deleted in colorectal cancer). *J Biol Chem* 2015;290:5783–5796.
- Bretscher A, Reczek D, Berryman M. Ezrin: a protein requiring conformational activation to link microfilaments to the plasma membrane in the assembly of cell surface structures. *J Cell Sci* 1997;110:3011–3018.
- Bretscher A. Purification of an 80,000-dalton protein that is a component of the isolated microvillus cytoskeleton, and its localization in nonmuscle cells. *J Cell Biol* 1983;97:425–432.
- Fukunaga Y, Liu H, Shimizu M, Komiya S, Kawasuji M, Nagafuchi A. Defining the roles of beta-catenin and plakoglobin in cell-cell adhesion: isolation of beta-catenin/plakoglobin-deficient F9 cells. *Cell Struct Funct* 2005;30:25–34.
- Fehon RG, McClatchey AI, Bretscher A. Organizing the cell cortex: the role of ERM proteins. *Nat Rev Mol Cell Biol* 2010;11:276–287.
- Saotome I, Curto M, McClatchey AI. Ezrin is essential for epithelial organization and villus morphogenesis in the developing intestine. *Dev Cell* 2004;6:855–864.
- Speck O, Hughes SC, Noren NK, Kulikauskas RM, Fehon RG. Moesin functions antagonistically to the Rho pathway to maintain epithelial integrity. *Nature* 2003;421:83–87.
- Hegmans JP, Bard MP, Hemmes A, Luider TM, Kleijmeer MJ, Prins JB, *et al*. Proteomic analysis of exosomes secreted by human mesothelioma cells. *Am J Pathol* 2004;164:1807–1815.
- Carpagnano GE, Foschino-Barbaro MP, Mulé G, Resta O, Tommasi S, Mangia A, *et al*. 3p microsatellite alterations in exhaled breath condensate from patients with non-small cell lung cancer. *Am J Respir Crit Care Med* 2005;172:738–744.

23. Reddel HK, Bateman ED, Becker A, Boulet LP, Cruz AA, Drazen JM, *et al.* A summary of the new GINA strategy: a roadmap to asthma control. *Eur Respir J* 2015;46:622–639.
24. Shaw DE, Sousa AR, Fowler SJ, Fleming LJ, Roberts G, Corfield J, *et al.*; U-BIOPRED Study Group. Clinical and inflammatory characteristics of the European U-BIOPRED adult severe asthma cohort. *Eur Respir J* 2015;46:1308–1321.
25. Daubeuf F, Frossard N. Acute asthma models to ovalbumin in the mouse. *Curr Protoc Mouse Biol* 2013;3:31–37.
26. Yang G, Volk A, Petley T, Emmell E, Giles-Komar J, Shang X, *et al.* Anti-IL-13 monoclonal antibody inhibits airway hyperresponsiveness, inflammation and airway remodeling. *Cytokine* 2004;28:224–232.
27. Lordan JL, Bucchieri F, Richter A, Konstantinidis A, Holloway JW, Thornber M, *et al.* Cooperative effects of Th2 cytokines and allergen on normal and asthmatic bronchial epithelial cells. *J Immunol* 2002; 169:407–414.
28. Wang Y, Jia M, Yan X, Cao L, Barnes PJ, Adcock IM, *et al.* Increased neutrophil gelatinase-associated lipocalin (NGAL) promotes airway remodelling in chronic obstructive pulmonary disease. *Clin Sci (Lond)* 2017;131:1147–1159.
29. Théry C, Amigorena S, Raposo G, Clayton A. Isolation and characterization of exosomes from cell culture supernatants and biological fluids. *Curr Protoc Cell Biol* 2006;3221–32229.
30. Chen HQ, Yang J, Zhang M, Zhou YK, Shen TY, Chu ZX, *et al.* *Lactobacillus plantarum* ameliorates colonic epithelial barrier dysfunction by modulating the apical junctional complex and PepT1 in IL-10 knockout mice. *Am J Physiol Gastrointest Liver Physiol* 2010; 299:G1287–G1297.
31. Wawrzyniak P, Wawrzyniak M, Wanke K, Sokolowska M, Bendelja K, Rückert B, *et al.* Regulation of bronchial epithelial barrier integrity by type 2 cytokines and histone deacetylases in asthmatic patients. *J Allergy Clin Immunol* 2017;139:93–103.
32. Ezzell RM, Chafel MM, Matsudaira PT. Differential localization of villin and fimbrin during development of the mouse visceral endoderm and intestinal epithelium. *Development* 1989;106:407–419.
33. Maunoury R, Robine S, Pringault E, Huet C, Guénet JL, Gaillard JA, *et al.* Villin expression in the visceral endoderm and in the gut anlage during early mouse embryogenesis. *EMBO J* 1988;7:3321–3329.
34. Bretscher A, Edwards K, Fehon RG. ERM proteins and merlin: integrators at the cell cortex. *Nat Rev Mol Cell Biol* 2002;3:586–599.
35. Hiscox S, Jiang WG. Ezrin regulates cell–cell and cell–matrix adhesion, a possible role with E-cadherin/beta-catenin. *J Cell Sci* 1999;112: 3081–3090.
36. Ren L, Hong SH, Cassavaugh J, Osborne T, Chou AJ, Kim SY, *et al.* The actin-cytoskeleton linker protein ezrin is regulated during osteosarcoma metastasis by PKC. *Oncogene* 2009;28:792–802.
37. Lan M, Kojima T, Murata M, Osanai M, Takano K, Chiba H, *et al.* Phosphorylation of ezrin enhances microvillus length via a p38 MAP-kinase pathway in an immortalized mouse hepatic cell line. *Exp Cell Res* 2006;312:111–120.
38. Parameswaran N, Eryindah-Asonye G, Bagheri N, Shah NB, Gupta N. Spatial coupling of JNK activation to the B cell antigen receptor by tyrosine-phosphorylated ezrin. *J Immunol* 2013;190:2017–2026.
39. Kelly-Welch AE, Hanson EM, Boothby MR, Keegan AD. Interleukin-4 and interleukin-13 signaling connections maps. *Science* 2003;300: 1527–1528.
40. Monni R, Haddaoui L, Naba A, Gallais I, Arpin M, Mayeux P, *et al.* Ezrin is a target for oncogenic Kit mutants in murine erythroleukemia. *Blood* 2008;111:3163–3172.
41. Wernig G, Kharas MG, Okabe R, Moore SA, Leeman DS, Cullen DE, *et al.* Efficacy of TG101348, a selective JAK2 inhibitor, in treatment of a murine model of JAK2V617F-induced polycythemia vera. *Cancer Cell* 2008;13:311–320.
42. Gomperts BN, Kim LJ, Flaherty SA, Hackett BP. IL-13 regulates cilia loss and foxj1 expression in human airway epithelium. *Am J Respir Cell Mol Biol* 2007;37:339–346.
43. Skowron-zwarg M, Boland S, Caruso N, Coraux C, Marano F, Tournier F. Interleukin-13 interferes with CFTR and AQP5 expression and localization during human airway epithelial cell differentiation. *Exp Cell Res* 2007;313:2695–2702.
44. Kulshreshtha A, Ahmad T, Agrawal A, Ghosh B. Proinflammatory role of epithelial cell-derived exosomes in allergic airway inflammation. *J Allergy Clin Immunol* 2013;131:1194–1203, 1203.e1–1203.e14.
45. Gatti JL, Métayer S, Belghazi M, Dacheux F, Dacheux JL. Identification, proteomic profiling, and origin of ram epididymal fluid exosome-like vesicles. *Biol Reprod* 2005;72:1452–1465.
46. Piehl LL, Fischman ML, Hellman U, Cisale H, Miranda PV. Boar seminal plasma exosomes: effect on sperm function and protein identification by sequencing. *Theriogenology* 2013;79:1071–1082.
47. Pastor MD, Nogal A, Molina-Pinelo S, Meléndez R, Salinas A, González De la Peña M, *et al.* Identification of proteomic signatures associated with lung cancer and COPD. *J Proteomics* 2013;89:227–237.
48. Matsumoto H. Serum periostin: a novel biomarker for asthma management. *Allergol Int* 2014;63:153–160.
49. Silkoff PE, Laviolette M, Singh D, FitzGerald JM, Kelsen S, Backer V, *et al.*; Airways Disease Endotyping for Personalized Therapeutics (ADEPT) study investigators. Identification of airway mucosal type 2 inflammation by using clinical biomarkers in asthmatic patients. *J Allergy Clin Immunol* 2017;140:710–719.
50. Cooper BG. An update on contraindications for lung function testing. *Thorax* 2011;66:714–723.